Materials Today Communications 7 (2016) 101–107

Contents lists available at ScienceDirect

Materials Today Communications

journal homepage: www.elsevier.com/locate/mtcomm

Fabrication of copper/single-walled carbon nanotube composite film with homogeneously dispersed nanotubes by electroless deposition

Susumu Arai [a,*], Takuma Osaki [a], Mitsuhito Hirota [b], Mitsugu Uejima [b]

[a] Department of Chemistry and Material Engineering, Faculty of Engineering, Shinshu University, 4-17-1 Wakasato, Nagano 380-8553, Japan
[b] Research & Development Center, Zeon Corporation, 1-2-1 Yako, Kawasaki, Kanagawa 210-9507, Japan

ARTICLE INFO

Article history:
Received 4 September 2015
Received in revised form 8 April 2016
Accepted 20 April 2016
Available online 21 April 2016

Keywords:
Single-walled carbon nanotube
Copper
Composite
Electroless deposition

ABSTRACT

Copper/single-walled carbon nanotube (SWCNT) composite films were fabricated by electroless deposition. The SWCNTs were formed using the water-assisted chemical vapor deposition method. To prepare copper/SWCNT composite plating baths with homogeneously dispersed SWCNTs, magnetic stirring, ultrasonic homogenization, and collision-type atomization were examined as mechanical methods for the disintegration of SWCNT bundles. Appropriate dispersants were added to the plating baths to avoid re-aggregation of the disintegrated SWCNTs. The degree of SWCNT dispersion in the copper/SWCNT composite plating bath was evaluated using a particle size analyzer, and the microstructures of the copper/SWCNT composite films were analyzed using scanning electron microscopy and X-ray diffraction. Collision-type atomization most significantly improved the degree of SWCNT dispersion in the composite plating bath. Using this treatment method, copper/SWCNT composite films with homogeneous dispersions of SWCNTs were successfully fabricated by electroless deposition.

1. Introduction

Carbon nanotubes (CNTs) [1,2] have excellent mechanical characteristics and high thermal conductivity. Consequently, research into practical applications of CNTs, including the preparation of resin/CNT, ceramic/CNT, and metal/CNT composites, has been actively pursued. CNTs also have an extremely high current-carrying capacity (ampacity) that is one thousand times higher than that of copper (10^9 A cm^{-2}) [3]; therefore, applications for power cables [4] and very-large-scale integration (VLSI) wiring [5] have been investigated. Subramaniam et al. reported that copper/single-walled carbon nanotube (SWCNT) composites exhibit both high electrical conductivity (similar to that of copper) and high ampacity [6]. They fabricated the copper/SWCNT composites by filling gaps in a horizontally aligned forest of SWCNTs with copper using electroplating techniques.

We have reported that copper/multi-walled carbon nanotube (MWCNT) composite films can be fabricated using a plating technique known as composite plating [7–13]. The copper/MWCNT composite films can be fabricated by both electrolytic composite plating [7–10] and electroless composite plating [11–13]. The latter technique enables the formation of copper/MWCNT composite films not only on electrically conductive substrates, but also on insulators such as resin. In CNT composite plating, CNTs are incorporated into a metal film during the metal deposition process; therefore, a homogeneous dispersion of CNTs in the composite plating bath is very important to form a homogeneous dispersion of CNTs in the metal/CNT composite film. CNTs are hydrophobic and plating baths are typically aqueous solutions; therefore, hydrophilic treatment of the CNTs is necessary to achieve adequate dispersion in the plating bath. The introduction of hydrophilic groups onto the surfaces of CNTs or the addition of appropriate surfactants is generally employed to hydrophilize CNTs. Acid treatment [14], heat treatment [15], and plasma treatment [16] are often used to graft hydrophilic groups, such as hydroxyl or carboxyl groups, onto the surfaces of CNTs; however, these treatments destroy the sp^2 carbon bonding of the CNTs. In contrast, hydrophilic treatment using dispersants does not damage CNTs, and various kinds of surfactants [17–34], such as sodium dodecyl sulfate (SDS), have been examined. We have fabricated copper/MWCNT composite films using composite plating baths in which MWCNTs are dispersed with appropriate dispersants. However, SWCNTs are the thinnest among the various types of CNTs and can thus easily form aggregates referred to as bundles. Therefore, to obtain copper/SWCNT composite films with a homogeneous dispersion of SWCNTs as the primary particles requires the preparation of a

* Corresponding author.
E-mail address: araisun@shinshu-u.ac.jp (S. Arai).

http://dx.doi.org/10.1016/j.mtcomm.2016.04.009

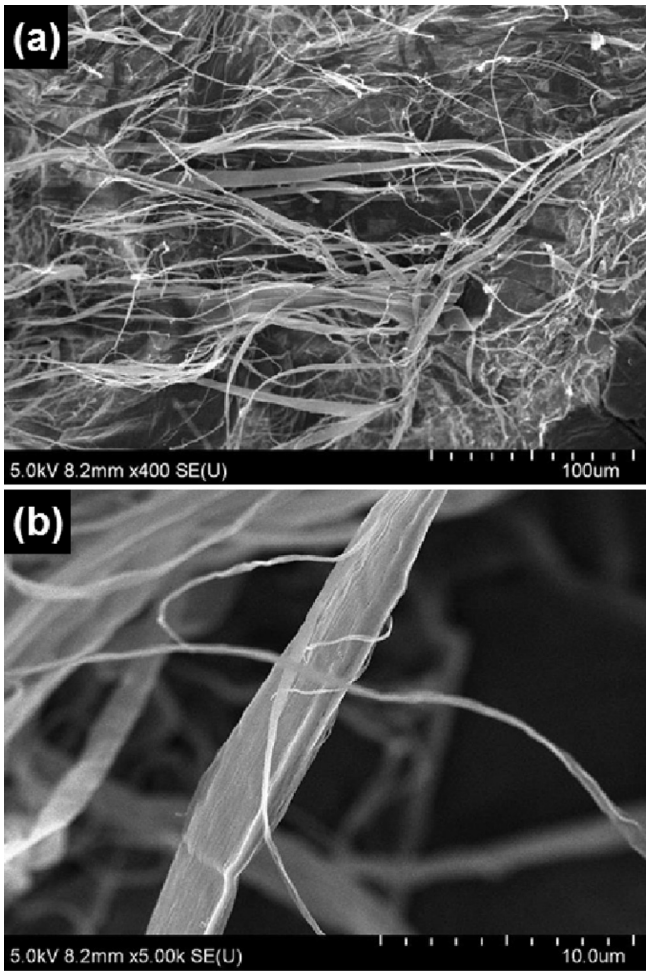

Fig. 1. (a) Low- and (b) high-magnification SEM images of the SWCNTs used in the present study.

composite plating bath that contains well disintegrated and well dispersed SWCNTs.

In this study, magnetic stirring, ultrasonic homogenization, and collision-type atomization for the mechanical disintegration of SWCNT bundles were examined to prepare composite plating baths with homogeneously dispersed SWCNTs. Copper/SWCNT composite plating films were then fabricated by electroless deposition using the prepared composite plating baths, and their microstructures were characterized.

2. Experimental

2.1. Chemicals

SWCNTs (Zeon Corp.) formed by the water-assisted chemical vapor deposition method [35], also known as the "super growth" method, were used in the present study. The microstructures of the SWCNTs were observed using field-emission scanning electron microscopy (FE-SEM; Hitachi SU-8000) and high resolution transmission electron microscopy (HRTEM; JEOL JSM-2100F). Fig. 1 shows SEM images of the SWCNTs used in this study. The SWCNTs form bundles (Fig. 1b) that are over 100 μm long (Fig. 1a). Fig. 2 shows TEM images of the SWCNTs, which have diameters of ca. 4 nm (Fig. 2a). TEM observations (Fig. 2b) also confirmed that the SWCNTs form bundles.

The $CuSO_4{\cdot}5H_2O$, ethylenediaminetetraacetic acid disodium salt dihydrate (EDTA $2Na{\cdot}2H_2O$), glyoxylic acid monohydrate

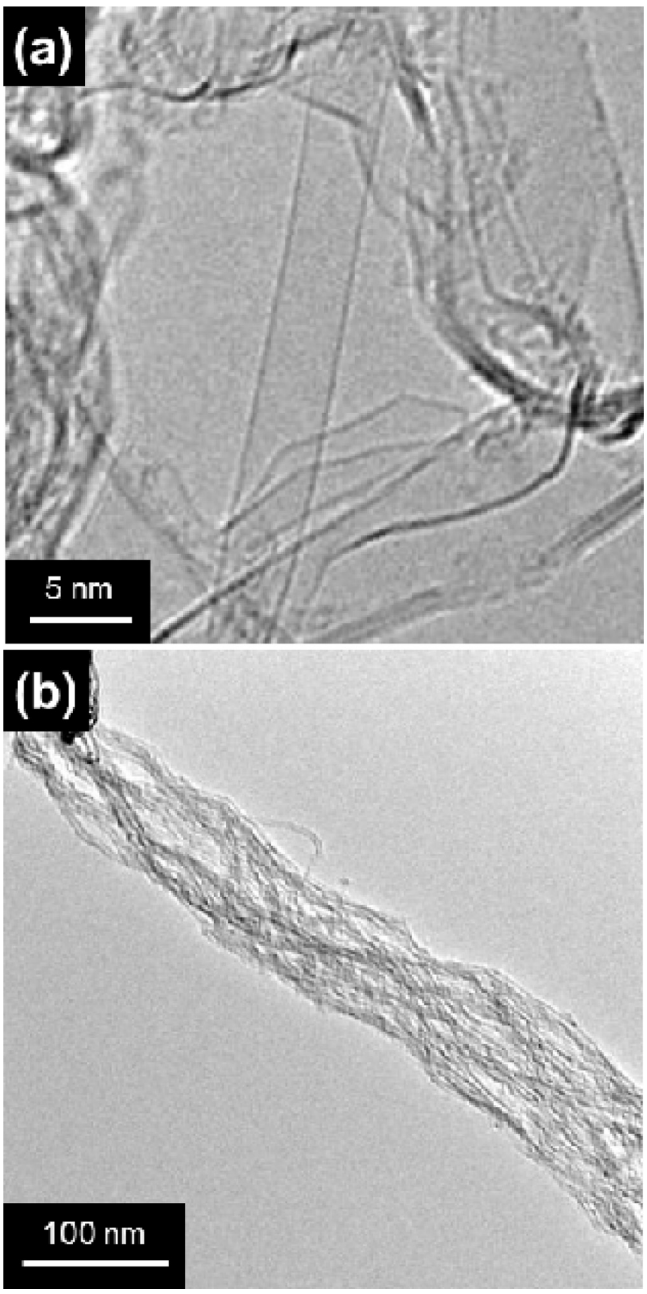

Fig. 2. TEM images of SWCNTs used in the present study. (a) single SWCNT, and (b) SWCNT bundle.

($CHOCOOH{\cdot}H_2O$), $SnCl_2{\cdot}H_2O$, $PdCl_2$, HCl, H_2SO_4, and KOH (Wako Pure Chemical Industries, Ltd.) used in this study were special grade reagents. Reagent grade SDS and hydroxypropyl cellulose (HPC; 2.0–2.9 mPa s, Wako Pure Chemical Industries, Ltd.) were used as SWCNT dispersants. Pure water from an electrodialysis water purifier (Advantec MFS, RFP343RA) was used in all experiments.

2.2. Composition of electroless copper/SWCNT composite plating bath

The composition of the electroless copper/SWCNT composite plating bath is given in Table 1 [13]. $CuSO_4{\cdot}5H_2O$, EDTA $2Na{\cdot}2H_2O$, and $CHOCOOH{\cdot}H_2O$ were used as a copper source, cuprous ion chelating agent, and cuprous ion reducing agent, respectively. SDS and HPC were used as the SWCNT dispersion agents.

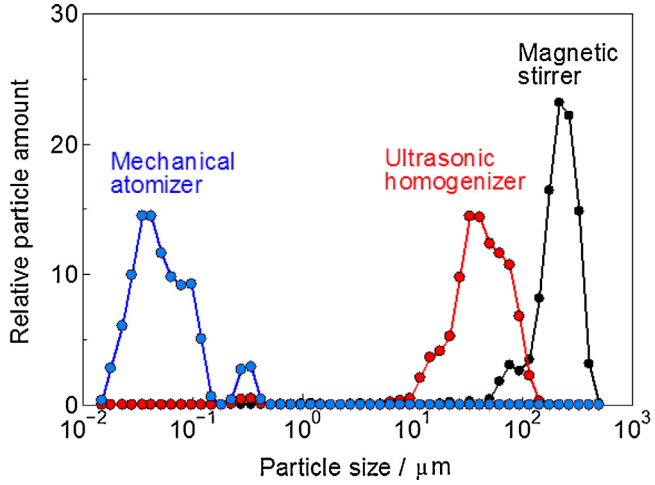

Fig. 3. Dispersibility of SWCNTs in the plating baths treated by various disintegration methods.

Table 1
Composition of copper/SWCNT composite plating bath.

Reagent	Concentration
$CuSO_4 \cdot 5H_2O$	0.06 M
EDTA 2Na·$2H_2O$	0.1 M
CHOCOOH·H_2O	0.03 M
SDS	1 g dm^{-3}
HPC	1 g dm^{-3}
SWCNTs	0.2 g dm^{-3}

2.3. Disintegration of SWCNT bundles in electroless copper/SWCNT composite plating bath

Without treatment, SWCNTs are present as bundles after being added to the plating baths (Fig. 1). Therefore, three mechanical methods, magnetic stirring, ultrasonic homogenization, and collision-type atomization, were examined to disintegrate the SWCNT bundles in the plating baths. Table 2 lists the details for each mechanical disintegration method. Mechanical atomization is a powerful disintegration method in which the dispersion liquids collide with each other. In the cases of magnetic stirring and ultrasonic homogenization, mechanical disintegration of the SWCNTs was directly applied to the plating baths. However, in the case of mechanical atomization, an aqueous solution of SWCNTs with SDS and HPC was first treated using the mechanical atomizer, and the SWCNT dispersion was then mixed with an aqueous solution containing $CuSO_4 \cdot 5H_2O$, EDTA 2Na·$2H_2O$, and CHOCOOH·H_2O to yield a plating bath with dispersed SWCNTs.

Table 2
Mechanical disintegration methods and operating conditions.

Method (apparatus)	Operating conditions
Magnetic stirrer (HPS-100: AS ONE Corp.)	800 rpm × 24 h
Ultrasonic homogenizer (US-300T: Nissei Corp.)	19.5 kHz, 300 W × 15 min
Mechanical atomizer (Star Burst Labo: Sugino Machine Ltd.)	245 MPa × 3 passes

2.4. Dispersibility of SWCNTs in plating baths

The dispersibility of SWCNTs in the plating baths was evaluated at room temperature using a laser diffraction particle analyzer (Shimadzu Seisakusho; SALD-7000). Measurements were conducted using plating baths without the CHOCOOH·H_2O reducing agent to avoid the copper deposition reaction during the measurements.

2.5. Fabrication of copper/SWCNT composite films by electroless deposition

Pure copper plates (JIS C1020P) with exposed surface areas of 10 cm^2 (3 × 3.3 cm) were used as substrates. Prior to electroless deposition, the substrates were immersed in a solution of 4.4×10^{-2} M $SnCl_2 \cdot 2H_2O$ + 0.12 M HCl at 30 °C for 6 min to allow the adsorption of Sn^{2+} ions (sensitization). The substrates were then immersed in a solution of 5.6×10^{-4} M $PdCl_2$ + 0.12 M HCl at 30 °C for 6 min to form catalytic palladium nuclei on the surfaces (activation). After the activation process, electroless plating was performed at 60 °C for 120 min with agitation by a stirrer.

2.6. Characterization of copper/SWCNT composite films by electroless deposition

The microstructure and morphology of the copper/SWCNT composite films were observed using FE-SEM. The phase structures of

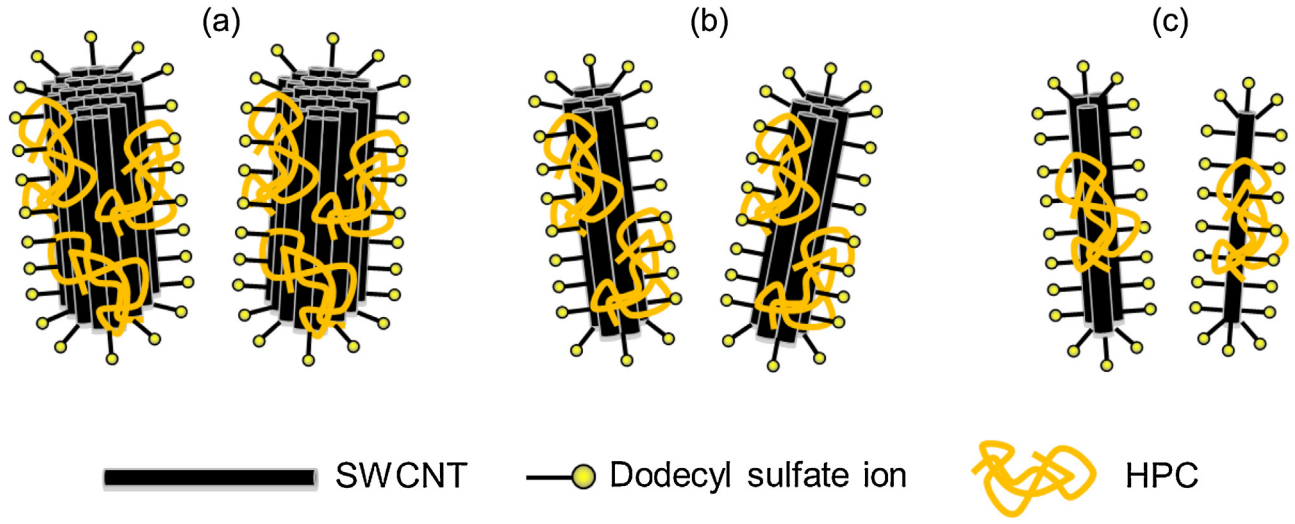

Fig. 4. Schematic representation of the different dispersion states of SWCNTs in the plating baths treated with (a) magnetic stirring, (b) ultrasonic homogenization, and (c) mechanical atomization.

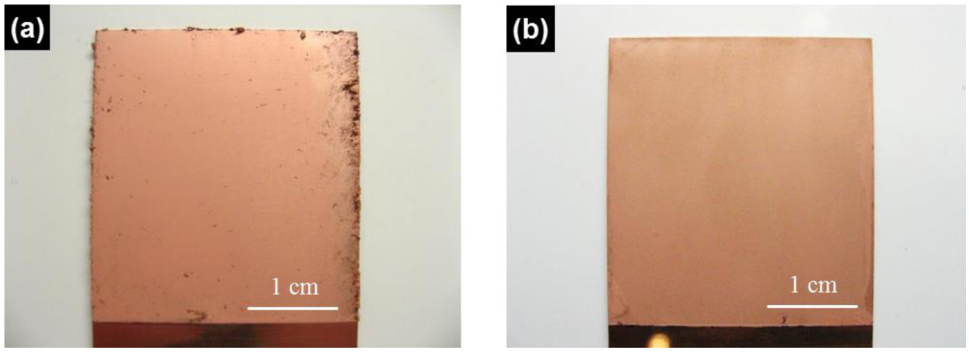

Fig. 5. Appearance of copper/SWCNT composite films deposited from the plating baths treated with (a) magnetic stirring and (b) mechanical atomization.

the composite films were examined using X-ray diffraction (XRD; Shimadzu Seisakusho, XRD-6000) with Cu $K_{\alpha 1}$ radiation.

3. Results and discussion

Fig. 3 shows a comparison of the dispersibility of the SWCNTs in the plating baths prepared by the different disintegration methods. For the laser diffraction particle size analysis, the particle shape was assumed to be spherical. In fact, because the SWCNTs are fiber-like and not spherical, the particle size in the figure does not accurately represent the diameter of the SWCNTs. However, the particle size distributions indicate the degree of dispersion of the SWCNTs. For disintegration with magnetic stirring, a large peak beyond 100 μm is observed, while a large peak around 50 μm is observed for disintegration with ultrasonic homogenization. In contrast, a large peak around 50 nm is observed for disintegration with mechanical atomization. These results show that the dispersibility increases in the order of magnetic stirring, ultrasonic homogenization, and mechanical atomization, with the latter being the most effective to disperse the SWCNTs in the plating bath.

The dispersion states of SWCNTs in the plating baths are schematically shown in Fig. 4, where the black sticks, black bars with yellow circles, and irregular orange lines represent single SWCNTs, dodecyl sulfate ions originating from SDS, and HPC molecules, respectively. The yellow circle of the dodecyl sulfate ion represents the sulfate group. Large SWCNT bundles are present in the plating bath treated with magnetic stirring. The SDS and HPC dispersants should be adsorbed onto the surfaces of the SWCNT bundles, which results in dispersion of these large SWCNT bundles (Fig. 4a). Medium-sized SWCNT bundles with adsorbed SDS and HPC should be present in the plating bath treated with ultrasonic homogenization (Fig. 4b). In the case of mechanical atomization, sufficiently disintegrated SWCNTs with adsorbed SDS and HPC should be present in the plating bath (Fig. 4c).

Fig. 5 shows the macroscopic appearance of films fabricated by electroless deposition. The external appearance of the films formed using the plating bath treated with magnetic stirring is not uniform (Fig. 5a). The color of the central region is reddish-brown, while the edge region is dark. In contrast, the films formed using the plating baths treated with the ultrasonic homogenizer and mechanical atomizer are relatively uniform and with the same reddish-brown color. The appearance of the film deposited using the bath treated using the mechanical atomizer is shown in Fig. 5b.

Fig. 6 shows surface SEM images of the dark edge region in Fig. 5a, where fibrous objects of around 100 μm in length are observed (Fig. 6a). The size of these fibrous objects is similar to that of the SWCNT bundles shown in Fig. 1a. Fig. 6b shows an enlarged SEM image of a fibrous object. Spherical particles of submicron size are observed on the fibrous object. Fig. 6c shows a high-magnification SEM image of Fig. 6b. Bundles of fibers that must be SWCNT bundles are observed with spherical particles on the surface of the bundles. When MWCNTs are incorporated into the deposited metal layer during MWCNT composite plating, metal is deposited not only on the deposited metal layer, but also on the edges or defect sites of MWCNTs protruding from the metal layer because the MWCNTs have electro-conductivity [36]. SWCNTs with armchair chirality have electro-conductivity and armchair type SWCNTs should be present in the SWCNT bundles; therefore, the spherical particles are considered to be copper particles deposited on the edges or defect sites of the electro-conductive SWCNTs incorporated in the deposited copper layer. Thus, in the case of magnetic stirring, large SWCNT bundles are incorporated into the deposited copper film at the edge region (Fig. 5a), probably because these large SWCNT bundles are easily caught at the edge of the substrate.

Fig. 7 shows surface SEM images of the central regions of the films formed from plating baths treated with the various disintegration methods. Fig. 7a shows a low-magnification SEM image of the film formed from the plating bath treated with magnetic stirring. No large SWCNT bundles are observed at the edge region (Fig. 6), and no SWCNTs are observed even at higher magnification (Fig. 7b). Fig. 7c shows a low-magnification SEM image of the film from the plating bath treated with ultrasonic homogenization, where no large SWCNT bundles are observed. However, thin fibrous objects that are considered to be thin SWCNT bundles of around 10–50 nm in diameter are observed at high magnification (Fig. 7d). These SWCNT bundles are incorporated relatively homogeneously, not only in the central region of the film, but also over the entire surface of the film. Fig. 7e shows a low-magnification SEM image of the film from the plating bath treated using mechanical atomization, where no large SWCNT bundles are observed. However, very thin fibrous objects that are considered to be SWCNTs with diameters of less than 10 nm are observed at high magnification (Fig. 7f). The diameters of the SWCNTs are around 4 nm, as shown in Fig. 2(a). Therefore, some of the CNTs incorporated in the copper film may be primary particles, which means that the SWCNTs in the plating bath treated with mechanical atomization are efficiently dispersed. These well-disintegrated and well-dispersed SWCNTs are incorporated homogeneously, not only in the central part of the film, but also over the entire surface of the film.

Fig. 8 shows XRD patterns for the copper/SWCNT composite films formed from the plating baths treated using the various disintegration methods. The diffraction peaks for all of the copper/SWCNT composite films can be assigned to face-centered-cubic copper. Since the three XRD patterns have similar peak intensity ratios, the different degrees of incorporation of SWCNTs in the copper films provided by the various disintegration methods does not significantly affect the crystal orientation of the copper films. In

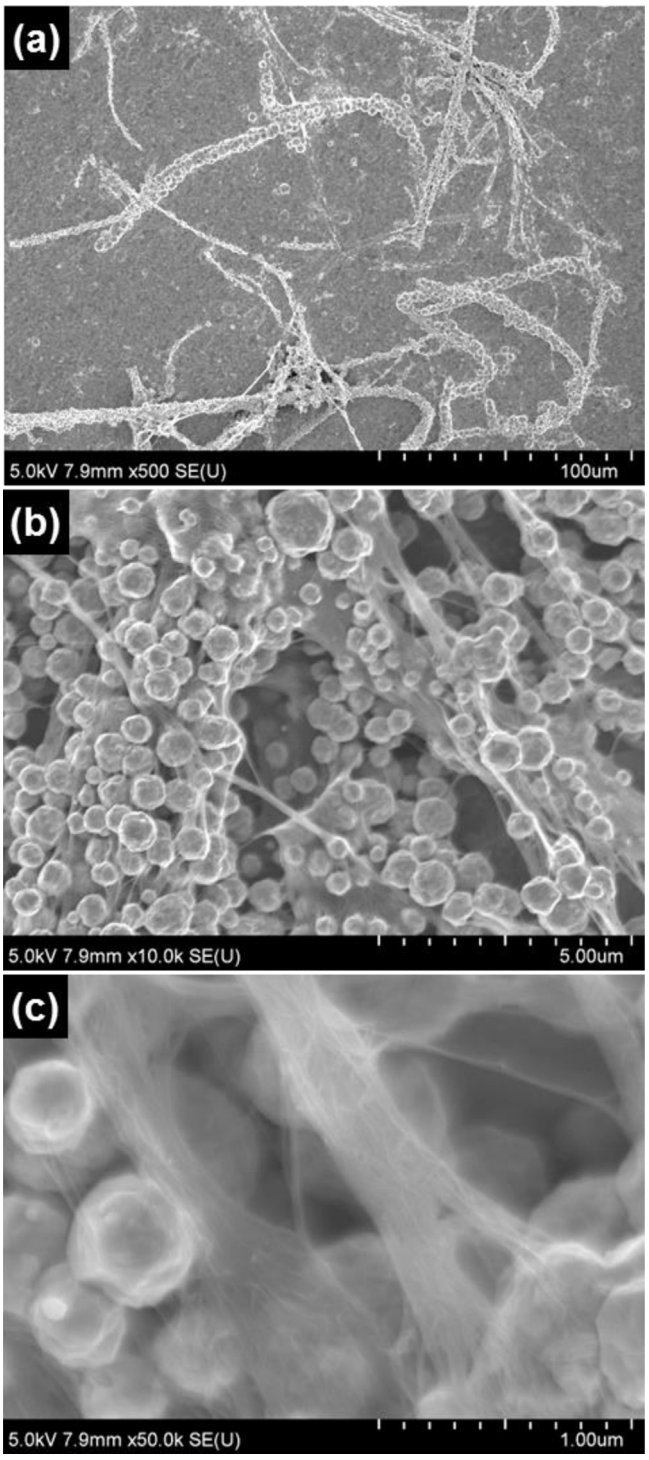

Fig. 6. Surface SEM images of the edge region of a copper/SWCNT composite film formed from a plating bath treated with magnetic stirring; (a) low magnification, (b) enlarged image of a fibrous object in (a), and high-magnification image of (b).

electroless copper plating, cuprous oxide (Cu_2O) is often formed in the copper film [37], which degrades properties such as the electrical or thermal conductivity of the copper film. The copper/MWCNT composite films formed from the plating bath treated using the mechanical atomizer contain a homogeneous distribution of SWCNTs without Cu_2O; therefore, such a composite film is expected to exhibit improved properties, such as thermal conductivity, compared to those of a pure copper film.

The properties of the copper/SWCNT composite film, such as the electrical and thermal conductivity, ampacity, and SWCNT content will be evaluated in future work.

4. Conclusions

Copper/SWCNT composite films were fabricated using an electroless deposition technique. A copper/SWCNT composite plating bath containing SDS and HPC as SWCNT dispersants

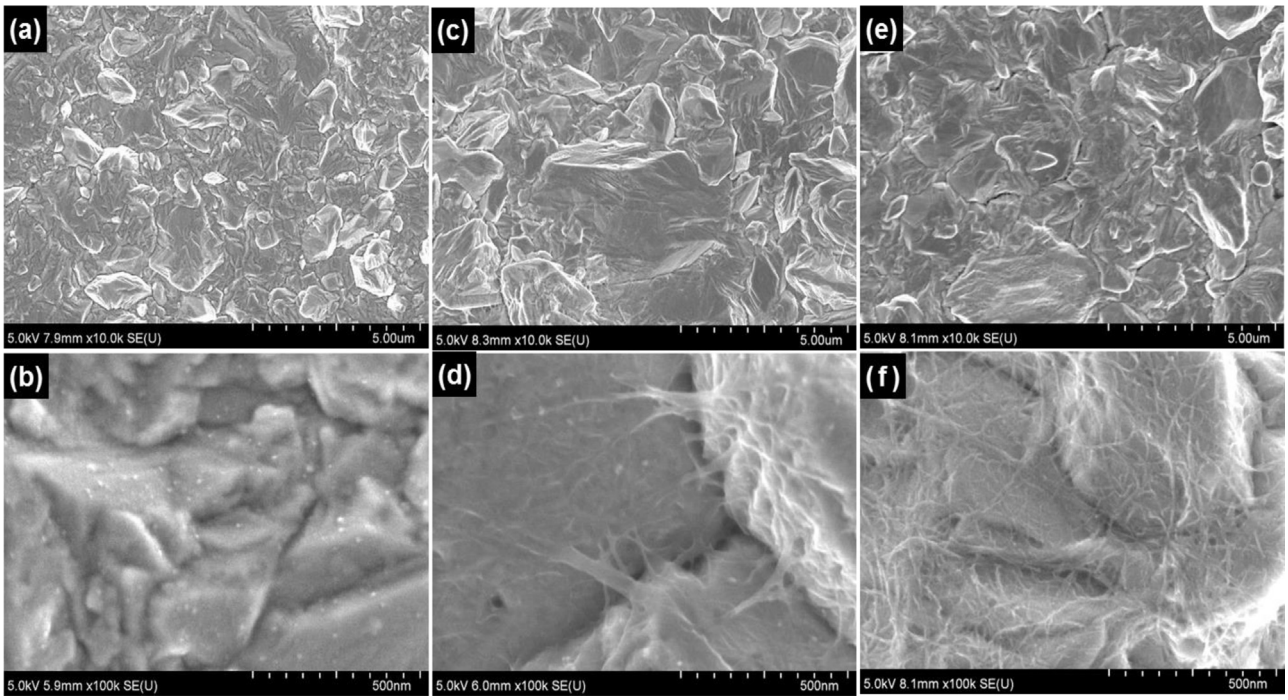

Fig. 7. Surface SEM images of central regions of copper/SWCNT composite films formed from plating baths treated by the various disintegration methods. (a) Low-magnification image/magnetic stirring, (b) high-magnification image of (a), (c) low-magnification image/ultrasonic homogenization, (d) high-magnification image of (c), (e) low-magnification image/mechanical atomization, and (f) high-magnification image of (e).

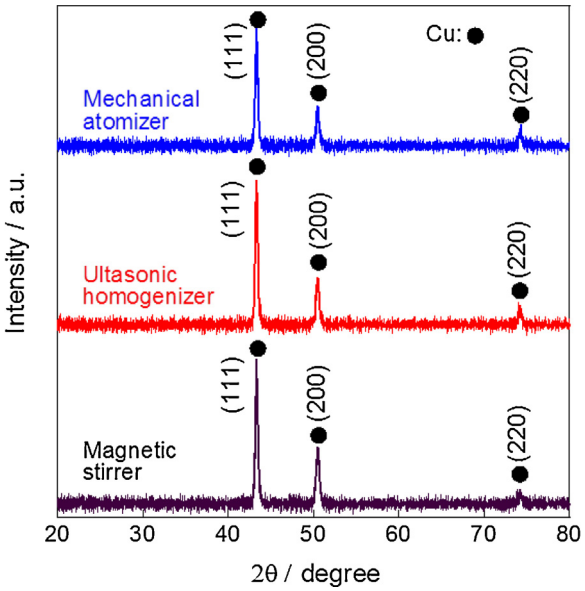

Fig. 8. XRD patterns for copper/SWCNT composite films formed from the plating baths treated by the various disintegration methods.

was employed. Various mechanical methods (magnetic stirring, ultrasonic homogenization, and mechanical atomization) were examined for disintegration of the SWCNT bundles in the plating baths. Magnetic stirring was not very effective, and a copper/SWCNT composite film containing large SWCNT bundles was formed. Ultrasonication produced relatively better results, and a copper/SWCNT composite film containing thin SWCNT bundles was formed. Mechanical atomization, in which the dispersion liquids collide with each other, yielded by far the best results, and was extremely effective at disintegration. Using this method, a copper/SWCNT composite film containing well-disintegrated and well-dispersed SWCNTs (single SWCNTs may be included) was successfully fabricated.

Acknowledgements

This work was supported by Grant-in Aid for Scientific Research (B) (No. 26289270) from the Japan Society for the Promotion of Science (JSPS). The authors thank Dr. H. Muramatsu of Shinshu University for conducting the TEM observations.

References

[1] A. Oberlin, M. Endo, T. Koyama, Filamentous growth of carbon through benzene decomposition, J. Cryst. Growth 32 (1976) 335–349.
[2] S. Iijima, T. Ichihashi, Single-shell carbon nanotubes of 1-nm diameter, Nature 363 (1993) 603–605.
[3] Z. Yao, C.L. Kane, C. Dekker, High-field electrical transport in single-wall carbon nanotubes, Phys. Rev. Lett. 84 (2000) 2941–2944.
[4] X. Wang, N. Behabtu, C.C. Young, D.E. Tsetalovich, M. Pasquali, J. Kone, High-ampacity power cables of tightly-packed and aligned carbon nanotubes, Adv. Funct. Mat. 24 (2014) 3241–3249.
[5] M. Horibe, M. Nihei, D. Kondo, A. Kawabata, Y. Awano, Carbon nanotube growth technologies using tantalum barrier layer for future ULSIs with Cu/low-k interconnect processes, Jpn. J. Appl. Phys. 44 (2005) 5309–5312.
[6] C. Subramaniam, T. Yamada, K. Kobayashi, A. Sekiguchi, D.N. Futaba, M. Yumura, K. Hata, One hundred fold increase in current carrying capacity in a carbon nanotube-copper composite, Nat. Commun. 4 (2013) 2202.
[7] S. Arai, M. Endo, Carbon nanofiber-copper composites fabricated by electroplating, Electrochem. Solid-State Lett. 7 (2004) C25–C26.
[8] S. Arai, M. Endo, Various carbon nanofiber-copper composite films prepared by electrodeposition, Electrochem. Commun. 7 (2005) 19–22.
[9] S. Arai, T. Saito, M. Endo, Cu-MWCNT composite films fabricated by electrodeposition, J. Electrochem. Soc. 157 (2010) D147–D153.
[10] S. Arai, T. Saito, M. Endo, Effects of additives on Cu-MWCNT composite plating films, J. Electrochem. Soc. 157 (2010) D127–D134.
[11] S. Arai, T. Kanazawa, Electroless deposition of Cu/multiwalled carbon nanotube composite films with improved frictional properties, ECS J. Solid State Sci. Technol. 3 (2014) P201–P206.
[12] S. Arai, T. Kanazawa, Electroless deposition and evaluation of Cu/multiwalled carbon nanotube composite films on acrylonitrile butadiene styrene resin, Surf. Coat. Technol. 254 (2014) 224–229.

[13] S. Arai, T. Osaki, Fabrication of copper/multiwalled carbon nanotube compoisites containing different sized nanotubes by electroless deposition, J. Electrochem. Soc. 162 (2015) D68–D73.
[14] K. Esumi, M. Ishigami, A. Nakajima, K. Sawada, H. Honda, Chemical treatment of carbon nanotubes, Carbon 33 (1995) 279–281.
[15] L. Jiang, L. Gao, Modified carbon nanotubes: an effective way to selective attachment of gold nanoparticles, Carbon 41 (2003) 2923–2929.
[16] Q. Chen, L. Dai, M. Gao, S. Huang, A. Mau, Plasma activation of carbon nanotubes for chemical modification, J. Phys. Chem. B 105 (2001) 618–622.
[17] B. Vigolo, A. Penicaud, C. Coulon, C. Sauder, R. Pailler, C. Journet, P. Bernier, P. Paulin, Macroscopic fibers and ribbons of oriented carbon nanotubes, Science 290 (2000) 1331–1334.
[18] M.J. O'Connell, S.M. Bachilo, C.B. Huffman, V.C. Moore, M.S. Strano, E.H. Haroz, K.L. Rialon, P.J. Boul, W.H. Noon, C. Kittrell, J. Ma, R.H. Hauge, R.B. Weisman, R.E. Smally, Band Gap Fluoresence from individual single-walled carbon nanotubes, Science 297 (2002) 593–596.
[19] C. Richard, F. Balavoine, P. Schultz, T.W. Ebbesen, C. Mioskowski, Supramolecular self-assembly of lipid derivatives on carbon nanotubes, Science 300 (2003) 775–778.
[20] M.F. Islam, E. Rojas, D.M. Bergey, A.T. Johnson, A.G. Yodh, High weight fraction surfactant solubilization of single-wall carbon nanotubes in water, Nano Lett. 3 (2003) 269–273.
[21] V.C. Moore, M.S. Strano, E.H. Haroz, R.H. Hauge, R.E. Smally, Nano Lett. 3 (2003) 1379–1382.
[22] L. Jiang, L. Gao, J. Sun, Production of aqueous colloidal dispersions of carbon nanotubes, J. Colloid Interface Sci. 260 (2003) 89–94.
[23] K. Yurekli, C.A. Mitchell, R. Krishnamoorti, Small-angle neutron scattering from surfactant-assisted aqueous dispersions of carbon nanotubes, J. Am. Chem. Soc. 126 (2004) 9902–9903.
[24] T. Hertel, A. Hagen, V. Talalaev, K. Arnold, F. Hennrich, M. Kappes, S. Rosenthal, J. McBride, H. Ulbricht, E. Flahaut, Spectroscopy of single- and double-wall carbon nanotubes environments, Nano Lett. 5 (2005) 511–514.
[25] J. Steinmetz, M. Glerup, M. Paillet, P. Bernier, M. Holzinger, Production of pure nanotube fibers using a modified wet-spinning method, Carbon 43 (2005) 2397–2429.
[26] Y. Tan, D.E. Resasco, Dispersion of single-walled carbon nanotubes of narrow diameter distribution, J. Phys. Chem. B 109 (2005) 14454–14460.
[27] N. Grossiord, P. van der Schoot, J. Meuldijk, C.E. Koning, Determination of the surface coverage of exfoliated carbon nanotubes by surfactant molecules in aqueous solution, Langmuir 23 (2007) 3646–3653.
[28] Z. Sun, V. Nicolosi, D. Rickard, S.D. Bergin, D. Aherne, J.N. Coleman, Quantitative evaluation of surfactant-stabilized single-walled carbon nanotubes: dispersion quality and its correlation with zeta potential, J. Phys. Chem. C 112 (2008) 10692–10699.
[29] A.J. Blanch, C.E. Lenehan, J.S. Quinton, Optimizing surfactant concentrations for dispersion of single-walled carbon nanotubes in aqueous solution, J. Phys. Chem. B 114 (2010) 9805–9811.
[30] W.H. Duan, Q. Wang, F. Collins, Dispersion of carbon nanotubes with SDS surfactants: a study from a binding energy perspective, Chem. Sci. 2 (2011) 1407–1413.
[31] J.N. Barisci, M. Tahhan, G.G. Wallace, S. Badaire, T. Vaugien, M. Maugey, P. Poulin, Properties of carbon nanotube fibers spun from DNA-stabilized dispersions, Adv. Funct. Mat. 14 (2004) 133–138.
[32] T. Takahashi, C.R. Luculescu, K. Uchida, T. Ishii, H. Yajima, Dispersion behavior and spectroscopic properties of single-walled carbon nanotubes in chitosan acidic aqueous solutions, Chem. Lett. 34 (2005) 1516–1517.
[33] Y. Yan, J. Cui, P. Potschke, Voit Brigitte, Dispersion of pristine single-walled carbon nanotubes using pyrene-capped polystyrene and its application for preparation of polystyrene matrix composites, Carbon 48 (2010) 2603–2612.
[34] B. Suarez, B.M. Simonet, S. Cardenas, M. Valcarcel, Separation of carbon nanotubes in aqueous medium by capillary electrophoresis, J. Chromagr. A 1128 (2006) 282–289.
[35] K. Hara, D.N. Futaba, K. Mizuno, T. Namai, M. Yumura, S. Iijima, Water-assisted highly efficient synthesis of impurity-free single-walled carbon nanotubes, Science 306 (2004) 1362–1364.
[36] S. Arai, M. Endo, N. Kaneko, Nickel-deposited multi-walled carbon nanotubes by electrodeposition, Carbon 42 (2004) 641–644.
[37] J. Shu, B.P.A. Grandjean, S. Kaliaguine, Effect of $Cu(OH)_2$ on electroless copper plating, Ind. Eng. Chem. Res. 26 (1997) 1632–1636.